

# Mathematical Model of a Three-Stage Innate Immune Response to a Pneumococcal Lung Infection

Amber M. Smith<sup>a,\*</sup>, Jonathan A. McCullers<sup>b</sup>, Frederick R. Adler<sup>c</sup>

<sup>a</sup>*Theoretical Biology and Biophysics, Los Alamos National Laboratory, Los Alamos, NM 87545, USA*

<sup>b</sup>*Department of Infectious Diseases, St. Jude Children's Research Hospital, Memphis, TN 38105, USA*

<sup>c</sup>*Departments of Mathematics and Biology, University of Utah, Salt Lake City, UT 84112, USA*

---

## Abstract

Pneumococcal pneumonia is a leading cause of death and a major source of human morbidity. The initial immune response plays a central role in determining the course and outcome of pneumococcal disease. We combine bacterial titer measurements from mice infected with *Streptococcus pneumoniae* with mathematical modeling to investigate the coordination of immune responses and the effects of initial inoculum on outcome. To evaluate the contributions of individual components, we systematically build a mathematical model from three subsystems that describe the succession of defensive cells in the lung: resident alveolar macrophages, neutrophils and monocyte-derived macrophages. The alveolar macrophage response, which can be modeled by a single differential equation, can by itself rapidly clear small initial numbers of pneumococci. Extending the model to include the neutrophil response required additional equations for recruitment cytokines and host cell status and damage. With these dynamics, two outcomes can be predicted: bacterial clearance or sustained bacterial growth. Finally, a model including monocyte-derived macrophage recruitment by neutrophils suggests that sustained bacterial growth is possible even in their presence. Our model quantifies the contributions of cytotoxicity and immune-mediated damage in pneumococcal pathogenesis.

*Keywords:* Bacterial Dynamics Model, *Streptococcus pneumoniae* Infection, Acute Inflammation, Dose-Dependence, Immune Response Modeling

---

\*Corresponding Author: Amber M. Smith

Address: Theoretical Biology and Biophysics, Los Alamos National Laboratory, Los Alamos, NM 87545, USA

Phone: 505-665-4662

Fax: 505-665-3493

e-mail: [asmith@lanl.gov](mailto:asmith@lanl.gov)

## 1. Introduction

*Streptococcus pneumoniae* (pneumococcus) is a common pathogen associated with community acquired pneumonia, bacterial meningitis, and secondary infections following influenza (World Health Organization, 2008). Furthermore, pneumococcus is the causative agent in an estimated one million deaths worldwide each year among children under 5 years of age (World Health Organization, 2008), particularly in developing countries. Although vaccination and antibiotic use have greatly reduced incidence of disease in all persons, the emergence of resistant strains coupled with an increase in incidence during influenza outbreaks (McCullers and English, 2008) has emphasized a need for novel treatments and a deeper understanding of pneumococcal infection kinetics.

Based on experimental studies in mice, this paper introduces a series of mathematical models that address the factors associated with favorable outcomes from pulmonary pneumococcal infections. These models track three stages of immune cell recruitment to identify how each cell type controls bacterial dynamics and the likelihood of host survival.

### 1.1. Innate Immune Response to *S. pneumoniae*

Pneumococci colonize the nasopharynx in up to 70% of young children (Giebink, 2001) and 40% of healthy adults (Austrian, 1986), and asymptomatic carriage may last up to 6 weeks in an individual (Orihuela and Tuomanen, 2006). However, pneumococci can migrate to the lungs resulting in a more serious infection. Nevertheless, only a small fraction of carriers develop pneumonia. The rarity of pneumococcal pneumonia in healthy individuals

reflects the efficiency of host defenses as most disease occurs when pathogen removal systems, such as ciliated epithelium and mucin entrapment, are compromised either due to preceding viral infections or underlying respiratory conditions (Kadioglu et al., 2008). In addition to host characteristics, both the pathogen strain and inoculum size determine whether a pneumococcal population can establish within a host (Kadioglu et al., 2008).

When host barriers are breached, three types of cells arrive sequentially and destroy pneumococci through phagocytosis: resident alveolar macrophages (AMs), neutrophils, and monocyte-derived macrophages (MDMs). Alveolar macrophages play an important role in the defense against airborne pathogens and provide the first line of cellular defense against a pneumococcal lung infection (Dockrell et al., 2003; Gwinn and Vallyathan, 2006; Taylor et al., 2005). These cells phagocytose bacteria that reach the terminal bronchioles and alveoli (Franke-Ullmann et al., 1996; Jonsson et al., 1985), and coordinate the innate immune response to infection (Kadioglu and Andrew, 2004; Knapp et al., 2003). It is thought that when the ratio of pneumococci to phagocytes does not exceed some critical, although unknown, number, AMs can successfully phagocytose and kill pneumococci (Knapp et al., 2003). However, as this ratio increases for larger initial pneumococcal inoculums, AMs are unable to eradicate all pneumococci. Alveolar macrophages also secrete proinflammatory cytokines, such as interleukin-1 (IL-1) and tumor necrosis factor alpha (TNF- $\alpha$ ), to initiate the inflammatory response and recruit activated neutrophils into the lung (Monton and Torres, 1998; Zhang et al., 2000).

With a high-dose challenge of pneumococci, neutrophils appear within 2-

4 hours postinoculation (pi) and dominate the initial inflammatory immune response. A rapid reduction of neutrophil numbers follows a peak 24-48 hours pi, even when bacterial titers remain high (Bergeron et al., 1998; Duong et al., 2001; Fillion et al., 2001; Kadioglu et al., 2000). This swift decrease in neutrophils is paralleled by MDM infiltration at 48 hours pi (Fillion et al., 2001). Nevertheless, pneumococcal growth can remain unbounded causing 100% mortality in mice within 5 days at higher inocula (Bergeron et al., 1998; Duong et al., 2001; Fillion et al., 2001), indicating a limit to the phagocytic capacity of all three types of cells (Clawson and Repine, 1976; Onofrio et al., 1983) and a potential for significant inflammation to occur.

These phenomena suggest that a three-stage phagocytic response is critical for clearance of larger inocula and that skewing of the innate response may have a profound impact on the outcome. Although it is known that effective phagocytosis is not the only factor determining pneumococcal pathogenesis, we aim here to capture some of the complexities of the innate immune response to pneumococcus by developing mathematical models for the three-stage phagocytic response and testing them with data on artificially infected mice.

### *1.2. Mathematical Models of Bacterial Kinetics*

Previously published mathematical models of bacterial kinetics and inflammatory processes present a conceptual framework to examine two phenomena of interest here (Lauffenburger, 1985; Pilyugin and Antia, 2000; Reynolds et al., 2006; Rudnev and Romanyukha, 1995): (i) the initial dose threshold, and (ii) the observed variations in outcome (clearance vs sustained growth). These studies (described below) use systems of ordinary differential



equations to describe bacterial pathogenesis and often divide phagocytic cells into a variety of different subpopulations. To address these behaviors, one study split the macrophage population into cells that are in a free state (i.e., not associated with bacteria) and cells that are engaged in active phagocytosis of bacteria (Pilyugin and Antia, 2000), and suggested that the “handling” time of bacteria limited the ability of macrophages to fully eradicate a bacterial population.

Other models include two separate subsets of phagocytes, neutrophils and macrophages (Lauffenburger, 1985; Rudnev and Romanyukha, 1995), and show that different behaviors are possible with various initial conditions. However, the models did not have these cells arriving sequentially, and the macrophage response included either only recruited macrophages (Rudnev and Romanyukha, 1995) or a single equation combining resident alveolar macrophages and MDMs (Lauffenburger, 1985). More commonly, however, models include only one subset of phagocytes. For example, a single type of macrophage was useful in a model that evaluated the importance of prolonged inflammation in the context of sepsis, and emphasized anti-inflammatory cytokines and tissue damage as the factors influencing infection outcomes (Reynolds et al., 2006).

Many of these models describe “generic” bacterial dynamics. However, differences among bacterial species render most prior formulations inappropriate for a pneumococcal lung infection. In particular, the succession of neutrophil and MDM accumulation depends on bacterial type and differs between various gram-positive bacteria and gram-negative bacteria (Schluger and Rom, 1997; Toews et al., 1979). For example, an infection with *Pseu-*

*Pseudomonas aeruginosa* (gram-negative) is similar to pneumococcus (gram-positive) in that neutrophils are the predominant phagocyte. However, neutrophils may appear simultaneously with MDMs during infections with *Klebsiella pneumoniae* (gram-negative) and *Staphylococcus aureus* (gram-positive) (Toews et al., 1979). This variation has been attributed to a distinct, but partially overlapping, set of cytokines induced by different species during bacterial colonization (Schluger and Rom, 1997).

Few existing models have sufficient experimental data for validation and parameterization, and no models specific to *S. pneumoniae* have been developed. We capitalize on the power and convenience of the mouse model system to compare the kinetics of three bacterial doses over the course of an infection and infer possible interactions between pneumococci and host immune responses. We infected groups of BALB/cJ mice with three different inocula of *S. pneumoniae* strain D39 and obtained bacterial measurements from the lungs of individual mice.

Using these data as a guideline, we develop mathematical models that describe the kinetics of each of the three stages. We find a single equation that characterizes the alveolar macrophage response, and use this equation to determine how an initial dose threshold arises. We then extend the model to incorporate proinflammatory cytokine production and the resulting neutrophil recruitment, and establish that two outcomes, clearance or sustained bacterial growth, are possible. Lastly, we examine the possibility of bacterial clearance given an influx of monocyte-derived macrophages. Through each of these models, we gain a better understanding of the extent to which AMs, neutrophils, MDMs, proinflammatory cytokines, and apoptotic cellular ma-

terial (“debris”) contribute to the initiation and resolution of a pneumococcal lung infection.

## 2. Experimental Data

### 2.1. Methods and Materials

#### 2.1.1. Mice

Adult (6-8 wk old) female BALB/cJ mice were obtained from Jackson Laboratories (Bar Harbor, ME). Mice were housed in groups of 4-6 mice in high-temperature 31.2 cm × 23.5 cm × 15.2 cm polycarbonate cages with isolator lids. Rooms used for housing mice were maintained on a 12:12-hour light:dark cycle at  $22 \pm 2^\circ\text{C}$  with a humidity of 50% in the biosafety level 2 facility at St. Jude Children’s Research Hospital (Memphis, TN). Prior to inclusion experiments, mice were allowed at least 7 days to acclimate to the animal facility. Laboratory Autoclavable Rodent Diet (PMI Nutrition International, St. Louis, MO) and autoclaved water were available ad libitum. All experiments were performed in accordance with the guidelines set forth by the Animal Care and Use Committee at St. Jude Children’s Research Hospital.

#### 2.1.2. Infectious Agents and Model

*S. pneumoniae* strain D39 (type 2) was transformed with the lux operon (Xenogen) (McCullers and Bartmess, 2003). For infection experiments, bacteria were diluted in sterile phosphate buffered saline (PBS) and administered at a dose of  $10^4$ ,  $10^5$  or  $10^6$  colony forming units (CFU) intranasally to groups of 6 mice lightly anesthetized with 2.5% inhaled isoflurane (Baxter, Deerfield,

IL) in a total volume of 100 $\mu$ l (50 $\mu$ l per nostril). Mice were weighed at the onset of infection and each subsequent day for illness and mortality.

### *2.1.3. Lung Titers*

Mice were euthanized by CO<sub>2</sub> asphyxiation. Lungs were aseptically harvested, washed three times in PBS, and placed in 500 $\mu$ l sterile PBS. Lungs were mechanically homogenized using the Ultra-Turrax T8 homogenizer (IKA-werke, Staufen, Germany). Lung homogenates were pelleted at 10,000 rpm for 5 minutes and the supernatants were used to determine the bacterial titer for each set of lungs using serial dilutions on tryptic soy-agar plates supplemented with 3% (vol/vol) sheep erythrocytes.

### *2.2. Experimental Results*

Infecting mice with an initial inoculum of 10<sup>4</sup> CFU resulted in undetectable bacterial lung titers 4 hours pi. We found that a dose above 10<sup>4</sup> CFU is necessary to induce a pneumococcal lung infection with the type 2 strain D39. The groups of mice given an initial dose of 10<sup>5</sup> CFU had bacterial titers initially increase exponentially for 8 hours, drop briefly at 16 hours pi then reach peaks up to 5.8  $\times$  10<sup>7</sup> CFU/ml lung homogenate at 24 hours pi. Bacterial lung titers then declined rapidly and, in all but one sample, became undetectable at 48 hours pi. All mice in the 72-hour group had completely cleared the infection (Figure 1).

Mice inoculated with 10<sup>6</sup> CFU had bacterial titers at significantly high levels by 4 hours pi, which reached peaks as high as 2.3  $\times$  10<sup>8</sup> CFU/ml lung homogenate by 16 hours pi. Titers began to decline thereafter; however, clearance slowed between 24 and 48 hours pi. The infection was not cleared

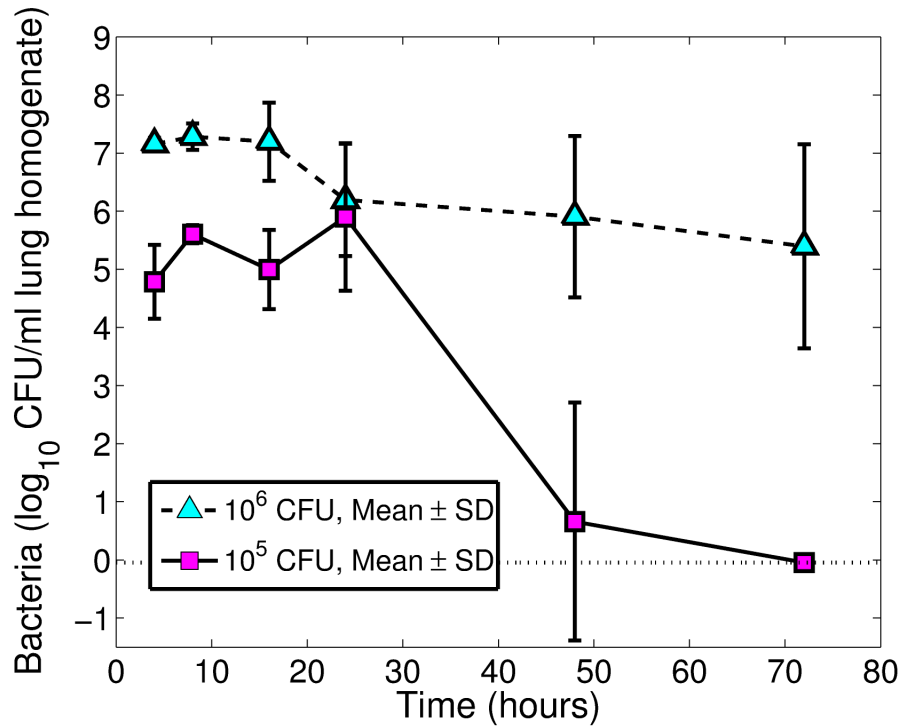


Figure 1: Pneumococcal lung titers (geometric means  $\pm$  SD) over time for groups of 6 mice inoculated with  $10^5$  (squares) or  $10^6$  (triangles) CFU. Titers for mice given  $10^4$  CFU were undetectable and are not shown. The dotted line represents a lower detection limit.

in these mice, which showed sustained bacterial titers 72 hours pi (Figure 1). Elevated bacterial titers over several days coupled with significant weight loss (data not shown) suggested these mice had severe pneumonia. All but one mouse (72-hour group) survived the experiment.

### 3. Mathematical Model

#### 3.1. Methods and Materials

Numerical simulation of model equations was done in Matlab using the ordinary differential equation (ODE) solver *ode45* for the alveolar macrophage

model and the neutrophil model, and using the delay differential equation (DDE) solver *dde23* for the monocyte-derived macrophage model. Parameter values used to simulate each model are given in Tables 1-3 and descriptions of the chosen values are given in the text.

### 3.2. Stage 1: The Alveolar Macrophage Response

Alveolar macrophages are part of the initial host defense that respiratory pathogens encounter when entering the airway. These cells are thought to tightly regulate growth of small pneumococcal populations but become insufficient with larger initial inocula. This limitation may explain the dependency of initial acquisition on inoculum size, as both we and others have found for a pulmonary pneumococcal infection (Sun and Metzger, 2008).

To investigate the dosage threshold, we developed a mathematical model (Equation (2)) that depicts the interaction between a pneumococcal population ( $P$ ) and the resident alveolar macrophages ( $M_A$ ). Pneumococci grow logistically at a rate  $r$  per hour with a maximum tissue carrying capacity,  $K_P$  CFU/ml, and are phagocytosed at rate  $\gamma_{M_A} f(P, M_A)$  per cell per hour, where

$$f(P, M_A) = \frac{n^x M_A}{P^x + n^x M_A}. \quad (1)$$

Equation (1) represents a decrease in phagocytosis with large pneumococcal population size. The shape parameter  $x$  describes the rate of consumption of pneumococci (Figure 2(a)). The value of  $n$  gives the ratio of bacteria to alveolar macrophages, with large values describing a higher phagocytosis rate

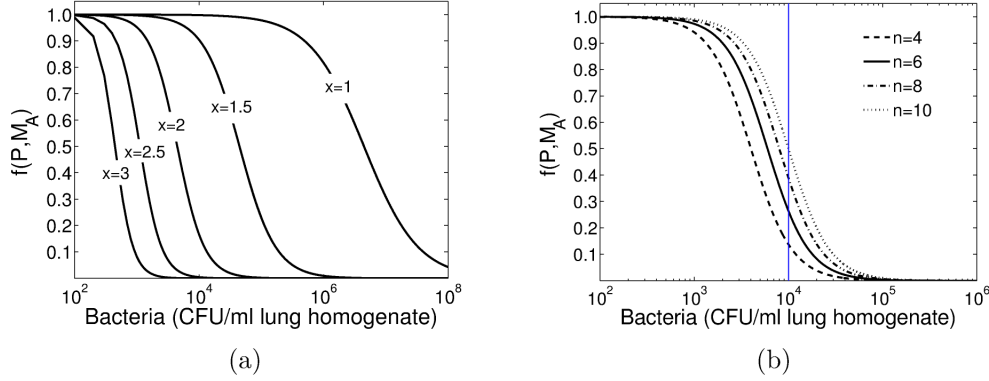


Figure 2: The function ( $f(P, M_A)$ ) describing the decrease in phagocytosis of pneumococcus by alveolar macrophages for various values of (a) the nonlinearity parameter  $x$ , and (b) the maximum number of pneumococci per alveolar macrophage,  $n$ . Vertical line at  $P(t) = 10^4$  shows the difference in  $f(P, M_A)$  given a particular value of  $n$ .  $M_A$  is fixed at  $10^6$  cells.

for a given inoculum size (Figure 2(b)).

Although alveolar macrophages were once thought to locally proliferate rather than derive from blood monocytes (Coggle and Tarling, 1982, 1984; Tarling et al., 1987), recent studies do not support this view (Murphy et al., 2008; Taut et al., 2008). We assume AMs are supplied at a constant rate of  $s$  cells per hour with a clearance rate  $d$ , for simplicity. We do not consider pneumococcal-induced death of AMs (Maus et al., 2004) as this effect would likely be minimal in the early stages of infection kinetics. Alveolar macrophage population dynamics are slow compared to bacterial clearance, so we take these cells to be in quasi-steady state such that  $M_A^* = s/d$ .

We term this model “the alveolar macrophage model”, which has dynamics described by a single equation for the pneumococcal population,





$$\frac{dP}{dt} = rP \left( 1 - \frac{P}{K_P} \right) - \gamma_{M_A} f(P, M_A^*) M_A^* P. \quad (2)$$

### 3.2.1. Parameter Identification

We did not use a sophisticated scheme to estimate parameter values because this model is designed to capture only the initial dose threshold and would fit at most 1-2 data points. We instead use parameter values available in the literature where possible and selected others to match the data by tuning values based on biologically feasible ranges (Table 1).

We set the steady state value of alveolar macrophages to  $M_A^* = 10^6$  cells, the estimated number that reside in a murine lung (van Oud Alblas and van Furth, 1979). Estimates of the turnover rate of alveolar macrophages range from 10-40 days (Coggle and Tarling, 1982; Godleski and Brain, 1972; van Oud Alblas and van Furth, 1979), although recent evidence suggests a longer life-span (Murphy et al., 2008). This corresponds to  $0.001 \leq d \leq 0.0042$  implying  $s = 1.0-4.2 \times 10^3$  cells per hour. Based on the maximum bacterial titer measured in our own experiment, we fix  $K_P = 2.3 \times 10^8$  CFU/ml.

The three initial values of pneumococci ( $P_0$ ) were chosen as  $10^3$ ,  $10^4$ , and  $10^5$  CFU/ml. The units of these values (CFU per ml of lung homogenate) differ from the units of initial inocula (CFU) used in the experiments. We assume only a portion of bacteria reach the lungs since some bacteria could be quickly trapped in the airway and removed by mucocilliary mechanisms. These values were chosen such that the data could be reproduced and to correspond to the three doses mice were infected with, i.e.,  $10^4$ ,  $10^5$ , and  $10^6$

CFU.

The doubling time of pneumococcal strain D39 is estimated to be 84 minutes when injected intravenously in a mouse model of sepsis (Benton et al., 1995). In contrast, the calculated doubling time in blood media is 20-30 minutes (Todar, 2002). Because we could not establish an exact value of the growth rate in the lung, we explored values between 20-84 minutes to determine which produced the best fit. We chose  $r = 11.3 \times 10^{-1}$  per hour, corresponding to a doubling time of approximately 37 minutes.

The maximum number of pneumococci associated with an alveolar macrophage ( $n$ ) was set to 5 CFU/ml per cell, based on a study that found, on average, 5 pneumococci bound to each human AM (Gordon et al., 2000) and since the lung homogenate is typically 1-1.5 ml. We fix the degree of nonlinearity ( $x$ ) in the function  $f(P, M_A)$  to a value of 2 based on our experimental findings that phagocytosis is decreased for initial inocula greater than  $10^4$  CFU (i.e.,  $10^3$  CFU/ml). Lastly, we found that  $\gamma_{M_A} = 5.6 \times 10^{-6}$  per cell per hour (i.e.,  $\gamma_{M_A} M_A = 5.6$  per hour) could predict the observed bacterial titers. We find this value reasonable as the estimated killing rate of *S. aureus* by neutrophils is 6.9 per hour (Hampton et al., 1994).

Table 1: The alveolar macrophage model (Stage 1) parameter definitions and values.

Parameter	Description	Units	Value	Comments
$r$	Bacterial growth rate	hour <sup>-1</sup>	$11.3 \times 10^{-1}$	see text
$K_P$	Bacterial carrying capacity	CFU/ml	$2.3 \times 10^8$	see text
$\gamma_{M_A}$	Bacterial clearance by AMs	cell <sup>-1</sup> hour <sup>-1</sup>	$5.6 \times 10^{-6}$	see text
$n$	Maximum number bacteria per AM	(CFU/ml)cell <sup>-1</sup>	5	(Gordon et al., 2000)
$x$	Nonlinearity in $f(P, M_A)$	N/A	2	see text
$s$	AM constant supply	cell <sup>-1</sup> hour <sup>-1</sup>	$1.0 - 4.2 \times 10^3$	see text
$d$	AM death rate	hour <sup>-1</sup>	$1.0 - 4.2 \times 10^{-3}$	(Coggle and Tarling, 1982; Godleski and Brain, 1972; van Oud Alblas and van Furth, 1979)
$M_A^*$	AM steady state value	cells	$10^6$	(van Oud Alblas and van Furth, 1979)
$P_0$	Initial number of pneumococci	CFU/ml	$10^3, 10^4, \text{ or } 10^5$	see text

### 3.2.2. Results - Alveolar Macrophage Model

We solved Equation (2) numerically with the parameter values specified in Table 1. For an initial pneumococcal value of  $P_0 = 10^3$  CFU/ml, the number of resident alveolar macrophages is large enough that bacterial titers decline immediately (Figure 3). A dose one log higher ( $P_0 = 10^4$  CFU/ml) results in a short lag ( $\sim 3$  hours) in bacterial growth as AMs initially limit exponential bacterial replication. Shortly after, however, pneumococci overwhelm the AM response and reach a steady-state value of  $P(t) = K_P$ . This slowed initial growth phase is not evident with a higher initial value ( $P_0 = 10^5$  CFU/ml) where immediate bacterial growth occurs.

These results imply that a decreased ability of resident alveolar macrophages to efficiently phagocytose large densities of pneumococci can produce a dosage threshold. Our model predicts that bacterial titers would quickly reach a maximum capacity which could then result in death of the host without additional components of the immune response.

### 3.3. Stage 2: The Neutrophil Response

Using the alveolar macrophage model, we found that resident alveolar macrophages could provide protection against a low-dose challenge of pneumococci, partial clearance of an intermediate dose, but no visible effects on a high-dose challenge (Figure 3). When AMs cannot control bacterial growth through phagocytosis, their main effect switches to modulating the inflammatory response by recruiting neutrophils to the infected lung (Jones et al., 2005; Mizgerd et al., 1996). We build upon Equation (2) to incorporate proinflammatory cytokine production that induces neutrophil migration and further phagocytosis of pneumococci.

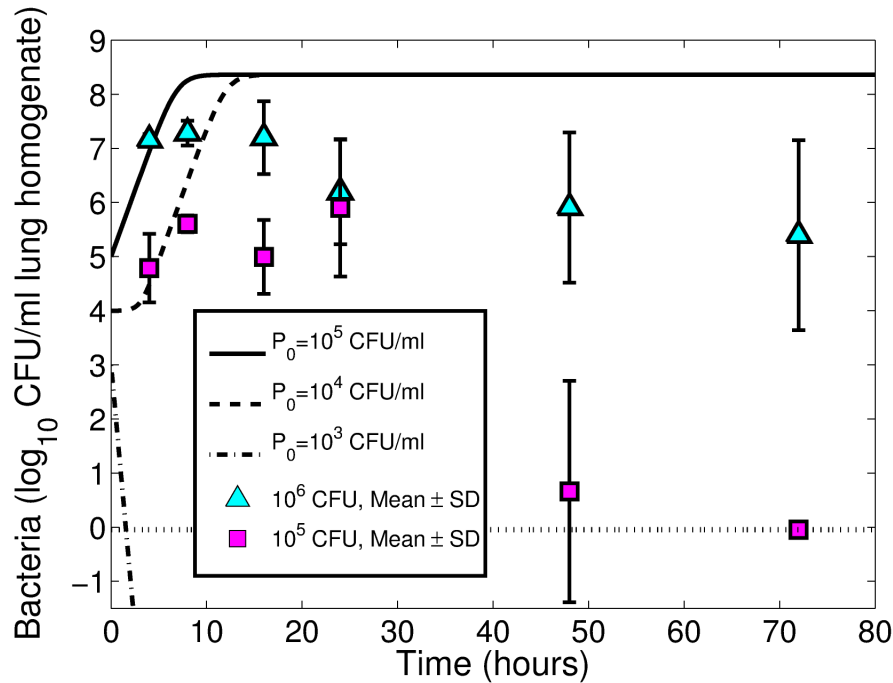


Figure 3: Numerical simulation of the alveolar macrophage model, Equation (2), using initial conditions  $P_0 = 10^3$  CFU/ml (dashed-dotted line),  $P_0 = 10^4$  CFU/ml (dashed line), and  $P_0 = 10^5$  CFU/ml (solid line). Pneumococcal titers (geometric means  $\pm$  SD) are shown for mice inoculated with  $10^5$  (squares) or  $10^6$  (triangles) CFU. Titers for mice given  $10^4$  CFU were undetectable and are not shown. The dotted line represents a lower detection limit.

### 3.3.1. Cytokine Production

Pneumococcal entry into the lung prompts the release of proinflammatory cytokines such as IL-1 and TNF- $\alpha$  (Bergeron et al., 1998). Alveolar macrophages produce a wide array of cytokines (Monton and Torres, 1998), and alveolar epithelial cells also secrete cytokines following pneumococcal attachment and/or cytotoxic injury (Maus et al., 2004; McRitchie et al., 2000; Stadnyk, 1994). Both IL-1 and TNF- $\alpha$  have been shown to increase rapidly during a pneumococcal infection, peaking 12 hours pi and then declining

(Bergeron et al., 1998).

Although these two cytokines have slightly different kinetics (Bergeron et al., 1998), we include both as the single variable  $C$  (Equation (9)). We divide the alveolar macrophage class into two subsets:  $M_R$ , representing AMs in a resting state that are not releasing cytokines, and  $M_C$ , representing AMs actively secreting cytokines. Alveolar macrophages in the  $M_R$  class become activated at rate  $\theta_M P$  due to interaction with bacteria and are deactivated at rate  $\kappa$  per hour. Equations (3)-(4) are the subsystem describing this process,

$$\frac{dM_R}{dt} = s - dM_R - \theta_M P M_R + \kappa M_C \quad (3)$$

$$\frac{dM_C}{dt} = \theta_M P M_R - \kappa M_C - dM_C. \quad (4)$$

We assume that the total AM population remains constant,  $M_A^* = M_R + M_C$ , and that the activation process is rapid when AMs encounter pneumococci. Thus, the number of alveolar macrophages that release cytokine is

$$M_C^* = \frac{\theta_M P M_A^*}{d + \kappa + \theta_M P}, \quad (5)$$

when we assume that the  $M_C$  population reaches a quasi-steady state. The rate of cytokine production from these cells is  $\nu$  pg/ml per hour.

To model cytokine production from tissue injury, we consider two populations of epithelial cells: target cells not associated with pneumococci ( $E_U$ , Equation (7)) and cells with pneumococci attached to cell surface receptors ( $E_A$ , Equation (8)). Following acute lung injury, little epithelial cell regen-

eration occurs within 3-5 days (Adamson et al., 1988; Ramphal et al., 1980), so we do not consider a source of new target cells. Pneumococci adhere to cells at a rate  $\omega P$  per hour. Cells with bacteria attached are lost, either from toxic effects of the bacteria or by immune-mediated mechanisms, at a rate  $d_E$  per hour. Cytokines are produced at a rate  $\alpha$  pg/ml per hour from epithelial cells and are degraded at a rate  $d_C$  per hour.

Antiinflammatory cytokines (e.g., IL-10) and other signaling molecules (e.g., nitric oxide (NO)) produced by alveolar macrophages and neutrophils during a pneumococcal infection aid regulation of the inflammatory process (Bergeron et al., 1998; Bingisser and Holt, 2001; Marriott et al., 2004; van der Poll et al., 1996; Thomassen et al., 1997). For simplicity, we do not explicitly include products such as IL-10 or NO in our model. Instead, we incorporate cytokine inhibition from neutrophil (N) effects by reducing production by a factor of  $1 + k_n N$ .

### 3.3.2. Neutrophil Recruitment

The signaling from proinflammatory cytokines recruits neutrophils ( $N$ , Equation (10)) at a rate  $\eta$  cells per pg/ml per hour which are then cleared at a rate  $d_N$  per hour. We do not include a limitation of the phagocytic rate ( $\gamma_N$ ) of neutrophils but we do set the maximum number of neutrophils present in the lung at  $N_{max}$ .

Neutrophil exposure to pneumococci results in apoptosis and, at high inocula, necrosis (Zysk et al., 2000). The effect of this process is two-fold. First, phagocyte apoptosis following bacterial colonization decreases inflammation and contributes to host recovery (DeLeo, 2004). Alveolar macrophages play an integral role in the clearance of the dead material and debris from the



airway (Dockrell et al., 2001, 2003). However, when apoptotic and necrotic material is not efficiently removed, tissue damage increases and bacterial growth may be increased.

We incorporate both the influence of pneumococcal-induced neutrophil apoptosis ( $d_{NP}$ ) and the role of alveolar macrophages in this process. To understand the effect of cell death on pathogenesis, we introduce a state variable to account for the accumulation of debris ( $D$ , Equation (11)), which has arbitrary units. In our model, neutrophil death, both natural and bacterial-induced, and the death of epithelial cells translate into debris at rates  $\rho_1$ ,  $\rho_2$  and  $\rho_3$  per cell, respectively. Alveolar macrophages then eliminate excess debris at a rate  $d_D$  per hour. While AMs are engaged in clearing the airway of dead material, we assume their ability to phagocytose pneumococci is inhibited by a factor  $1 + k_d DM_A^*$ .

Together, these dynamics result in “the neutrophil model” given by

$$\frac{dP}{dt} = rP \left(1 - \frac{P}{K_P}\right) - \frac{\gamma_{MA} f(P, M_A^*)}{1 + k_d DM_A^*} M_A^* P - \gamma_N NP \quad (6)$$

$$\frac{dE_U}{dt} = -\omega P E_U \quad (7)$$

$$\frac{dE_A}{dt} = \omega P E_U - d_E E_A \quad (8)$$

$$\frac{dC}{dt} = \alpha \frac{E_A}{1 + k_n N} + \nu \frac{\theta_M P M_A^*}{(d + \kappa + \theta_M P)(1 + k_n N)} - d_C C \quad (9)$$

$$\frac{dN}{dt} = \eta C \left(1 - \frac{N}{N_{max}}\right) - d_{NP} NP - d_N N \quad (10)$$

$$\frac{dD}{dt} = \rho_1 d_{NP} NP + \rho_2 d_N N + \rho_3 d_E E_A - d_D DM_A^*. \quad (11)$$

### 3.3.3. Results - Neutrophil Model

The large number of parameters in our model restricts our ability to fit Equations (6)-(11) to the data. Therefore, most parameter values were chosen based on searches in biologically realistic ranges that matched the data, although we fix some values ( $d_C$  and  $d_N$ ) based on estimates reported in the literature (Gloff and Wills, 1992; Malech, 2007). The initial number of epithelial cells was set at  $E_U(0) = 10^8$  cells, based on a calculation of the number of cells residing in the murine lung (Stone et al., 1992), and the initial values of the remaining state variables ( $C$ ,  $N$ , and  $D$ ) were set to zero. All other parameter values are listed in Table 2.

Simulating Equations (6)-(11) with three different initial pneumococcal conditions ( $10^3$ ,  $10^4$  and  $10^5$  CFU/ml) shows three distinct outcomes (Figure 4a). A low dose,  $P_0 = 10^3$  CFU/ml, is immediately cleared by alveolar macrophages and does not result in noticeable cytokine production or neutrophil recruitment (Figure 4c,b).

Table 2: The neutrophil model (Stage 2) parameter definitions and values.

Parameter	Description	Units	Value	Comments
$\gamma_N$	Bacterial clearance by neutrophils	$\text{cell}^{-1}\text{hour}^{-1}$	$1.0 \times 10^{-5}$	see text
$\theta_M$	Activation of cytokine production	$(\text{CFU}/\text{ml})^{-1}\text{hour}^{-1}$	$4.2 \times 10^{-8}$	see text
$\kappa$	Deactivation of cytokine production	$\text{hour}^{-1}$	$4.2 \times 10^{-2}$	see text
$\nu$	Cytokine production by AMs	$(\text{pg}/\text{ml})\text{cell}^{-1}\text{hour}^{-1}$	$2.9 \times 10^{-2}$	see text
$\omega$	Bacterial attachment to epithelial cells	$(\text{CFU}/\text{ml})^{-1}\text{hour}^{-1}$	$2.1 \times 10^{-8}$	see text
$d_E$	Epithelial cell death	$\text{hour}^{-1}$	$16.7 \times 10^{-2}$	see text
$\alpha$	Cytokine production by epithelial cells	$(\text{pg}/\text{ml})\text{cell}^{-1}\text{hour}^{-1}$	$2.1 \times 10^{-2}$	see text
$k_n$	Cytokine inhibition by neutrophils	$\text{cell}^{-1}$	$1.4 \times 10^{-5}$	see text
$d_C$	Cytokine degradation rate	$\text{hour}^{-1}$	$8.3 \times 10^{-1}$	(Gloff and Wills, 1992)
$N_{max}$	Maximum number neutrophils	cells	$1.8 \times 10^5$	see text
$\eta$	Neutrophil recruitment rate	$\text{cells} (\text{pg}/\text{ml})^{-1}\text{hour}^{-1}$	$13.3 \times 10^{-1}$	see text
$d_N$	Neutrophil clearance rate	$\text{hour}^{-1}$	$6.3 \times 10^{-2}$	(Malech, 2007)
$d_{NP}$	Bacterial-induced death neutrophils	$(\text{CFU}/\text{ml})^{-1}\text{hour}^{-1}$	$2.5 \times 10^{-7}$	see text
$\rho_1$	Debris from bacterial-induced neutrophil death	$\text{cell}^{-1}$	$1.0 \times 10^{-1}$	see text
$\rho_2$	Debris from neutrophil death	$\text{cell}^{-1}$	$1.0 \times 10^{-3}$	see text
$\rho_3$	Debris from epithelial cell death	$\text{cell}^{-1}$	$1.0 \times 10^{-5}$	see text
$d_D$	Removal of debris by AMs	$\text{cell}^{-1}$	$2.5 \times 10^{-6}$	see text
$k_d$	Phagocytosis inhibition	$\text{cell}^{-1}$	$5.0 \times 10^{-9}$	see text

Table 2 – Continued

Parameter	Description	Units	Value	Comments
$P(0)$	Initial number of pneumococci	CFU/ml	$10^3, 10^4$ or $10^5$	see text
$E_U(0)$	Initial number of epithelial cells	cells	$10^8$	(Stone et al., 1992)
$E_A(0)$	Initial number of epithelial cells with bacteria	cells	0	see text
$C(0)$	Initial concentration	pg/ml	0	see text
$N(0)$	Initial number of neutrophils	cells	0	see text
$D(0)$	Initial amount of debris	N/A	0	see text

At an intermediate value ( $P_0 = 10^4$  CFU/ml), the lag in bacterial growth initially from clearance by alveolar macrophages is reinforced by the appearance of neutrophils in the lung, which extends the delay in exponential bacterial growth from 3 hours to 6 hours (Figure 4a). Proinflammatory cytokine production is initially slow but increases rapidly thereafter and reaches a peak 24 hours pi (Figure 4c). These dynamics agree with experimental measurements of both IL-1 and TNF- $\alpha$  (Bergeron et al., 1998). Paralleling cytokine dynamics, neutrophils increase rapidly and peak 36 hours pi before slowly declining over several days (Figure 4b), also consistent with empirical observations (Fillion et al., 2001). The migration of neutrophils into the infection site effectively controls bacterial growth, which peaks 16 hours pi. Elimination of bacteria slows between 48-72 hours pi corresponding to a decrease in neutrophil numbers. At this time, alveolar macrophages are freed up from debris removal and return to phagocytosis of pneumococci. It is unclear whether or not this occurs biologically; however, it is possible that AMs are responsible for the completion of bacterial eradication. During the course of the infection, only a fraction ( $\sim 65\%$ ) of epithelial cells are killed as a result of bacterial adherence (Figure 4e,f).

The neutrophil response is not sufficient to clear a high dose inoculation. For  $P_0 = 10^5$  CFU/ml, bacterial growth slows briefly within 3 hours pi in accordance with a sharp rise in both neutrophils and proinflammatory cytokine concentration (Figure 4a,b,c). However, pneumococcal-induced neutrophil apoptosis results in an equally sharp decrease of these phagocytes. At this

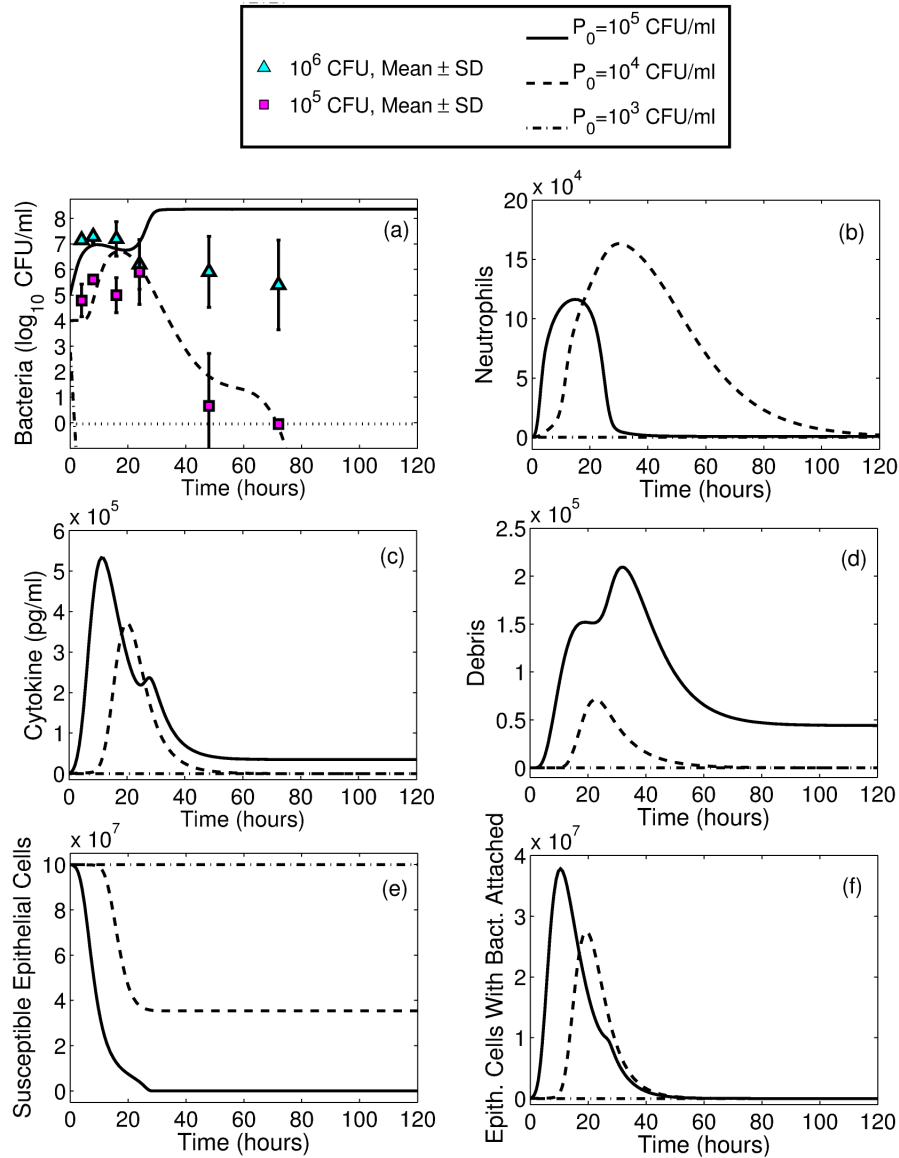


Figure 4: Numerical simulation of the neutrophil model, Equations (6)-(11), using initial conditions  $P_0 = 10^3$  CFU/ml (dashed-dotted line),  $P_0 = 10^4$  CFU/ml (dashed line),  $P_0 = 10^5$  CFU/ml (solid line), and parameter values in Table 2. (a) Bacteria against titer data (squares -  $10^5$  CFU/mouse, triangles -  $10^6$  CFU/mouse), (b) neutrophils, (c) proinflammatory cytokine, (d) debris, (e) susceptible epithelial cells, and (f) epithelial cells with bacteria attached.

point, 24 hours pi, bacterial titers rise quickly and reach the maximum tissue carrying capacity ( $K_P$ ). In addition, a significant amount of debris results from both the cytotoxic effects on neutrophils and epithelial cells. In this case, all target cells are killed by pneumococcal attachment.

We next simulated Equations (6)-(11) with additional values of  $P_0$  to determine the extent to which outcomes are altered with small changes in the initial condition. As illustrated in Figure 5, the alveolar macrophage response is sufficient for all initial values under  $P_0 = 10^4$  CFU/ml and bacterial titers decline rapidly. However, for initial conditions larger than  $P_0 = 10^4$  CFU/ml, bacteria grow exponentially with an evident lag phase in only a small region around this value. The length of time that bacterial growth is controlled by neutrophils decreases as  $P_0$  increases, with complete clearance possible below some critical value of  $P_0$  ( $3.98 \times 10^4$  CFU/ml, compared to  $9.99 \times 10^3$  with AMs only). These dynamics correspond to an unstable equilibrium between  $P(t) = 0$  and  $P(t) = K_P$ , although we were not able to find this value analytically.

#### 3.4. Stage 3: The Monocyte-Derived Macrophage Response

Although neutrophils dominate the early cellular influx of leukocytes (i.e., white blood cells) into sites of pulmonary pneumococcal infections (Mizgerd et al., 1996), these cells are replaced by monocyte-derived macrophages later during inflammation (Fillion et al., 2001). The shift to MDM recruitment is thought to be triggered by the release of soluble factors from neutrophils



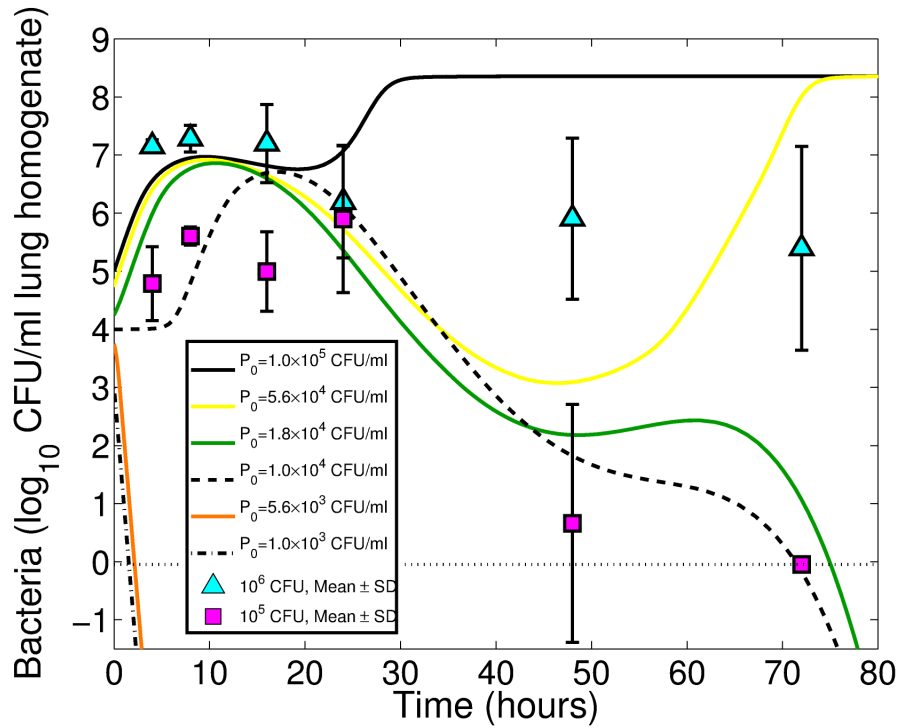


Figure 5: Numerical simulation of the neutrophil model, Equations (6)-(11), with the parameter values in Table 2 and various initial values of bacteria:  $P_0 = 10^3$  CFU/ml (dashed-dotted line),  $P_0 = 5.6 \times 10^3$  CFU/ml (solid orange line),  $P_0 = 10^4$  CFU/ml (dashed line),  $P_0 = 1.8 \times 10^4$  CFU/ml (solid green line),  $P_0 = 5.6 \times 10^4$  CFU/ml (solid yellow line),  $P_0 = 10^5$  CFU/ml (solid black line), and parameter values in Table 2.

(Doherty et al., 1988). However, other studies suggest the switch may be the result of MDM response to chemokines produced by tissue cells (Henderson et al., 2003) or regulation by the cytokine IL-6 (Kaplanski et al., 2003). The delayed appearance of MDMs also correlates with macrophage-colony protein 1 (MCP-1) production (Fillion et al., 2001), NO release (Bergeron et al., 1998), and bacterial formyl peptide production (Fillion et al., 2001), many of which are either influenced by or directly produced by neutrophils

(Cassatella, 1995).

Rather than including the dynamics of cytokines such as IL-6, MCP-1, or NO, we assume MDM recruitment is proportional to the neutrophil population. Furthermore, we found it beneficial to assume that MDMs appear  $\tau$  time units after neutrophils at a rate  $\xi$  per hour, where the number of macrophages cannot exceed  $M_{max}$  (Equation (18)). Clearance of these cells occurs at a rate  $d_m$  per hour. We exclude macrophage apoptosis in response to the bacterial challenge since it has been shown to be delayed (Dockrell et al., 2001; Marriott et al., 2004). We also exclude the contribution of macrophage death to debris assuming that the effect is small. Recruited macrophages phagocytose pneumococci at a rate  $\gamma_m$  per cell per hour. Combining these dynamics with Equations (6)-(10) results in “the monocyte-derived macrophage model” which describes all three stages of phagocytosis,

$$\frac{dP}{dt} = rP \left( 1 - \frac{P}{K_P} \right) - \frac{\gamma_{M_A} f(P, M_A^*)}{1 + k_d D M_A^*} M_A^* P - \gamma_N N P - \gamma_m M P \quad (12)$$

$$\frac{dE_U}{dt} = -\omega P E_U \quad (13)$$

$$\frac{dE_A}{dt} = \omega P E_U - d_E E_A \quad (14)$$

$$\frac{dC}{dt} = \alpha \frac{E_A}{1 + k_n N} + \nu \frac{\theta_M P M_A^*}{(d + \kappa + \theta_M P)(1 + k_n N)} - d_C C \quad (15)$$

$$\frac{dN}{dt} = \eta C \left( 1 - \frac{N}{N_{max}} \right) - d_N N - d_{NP} N P \quad (16)$$

$$\frac{dD}{dt} = \rho_1 d_{NP} N P + \rho_2 d_N N + \rho_3 d_E E_A - d_D D M_A^* \quad (17)$$

$$\frac{dM}{dt} = \xi N(t - \tau) \left(1 - \frac{M}{M_{max}}\right) - d_m M. \quad (18)$$

### 3.4.1. Results - Monocyte-Derived Macrophage Model

With parameters in Table 3, this model exhibits the observed behavior of bacterial kinetics for all three initial conditions of pneumococci (Figure 6a). Recruited macrophages (Figure 6d) are evident starting at 24 hours pi and peak between 72 and 96 hours pi for an intermediate initial value of pneumococci ( $10^4$  CFU/ml). This is consistent with experimental findings (Fillion et al., 2001) and corresponds to successful elimination of bacteria, which occurs 24 hours earlier with these cells present than with neutrophils and AMs only. Furthermore, the threshold value of  $P_0$  such that bacterial eradication occurs is 2.5 times more when macrophages are recruited than with neutrophils and AMs only ( $9.97 \times 10^4$  vs  $3.98 \times 10^4$  CFU/ml). For high initial

Table 3: The monocyte-derived macrophage model (Stage 3) parameter definitions and values.

Parameter	Description	Units	Value
$\gamma_m$	Bacterial clearance by MDMs	cell <sup>-1</sup> hour <sup>-1</sup>	$3.2 \times 10^{-5}$
$M_{max}$	Maximum number of MDMs	cells	$1.8 \times 10^5$
$\xi$	MDM recruitment rate	hour <sup>-1</sup>	$3.8 \times 10^{-3}$
$d_m$	MDM clearance rate	hour <sup>-1</sup>	$1.9 \times 10^{-3}$
$\tau$	Time delay before MDM recruitment	hours	12
$M(0)$	Initial number of MDMs	cells	0
$N(t)$	Number of neutrophils for $-\tau < t \leq 0$	cells	0

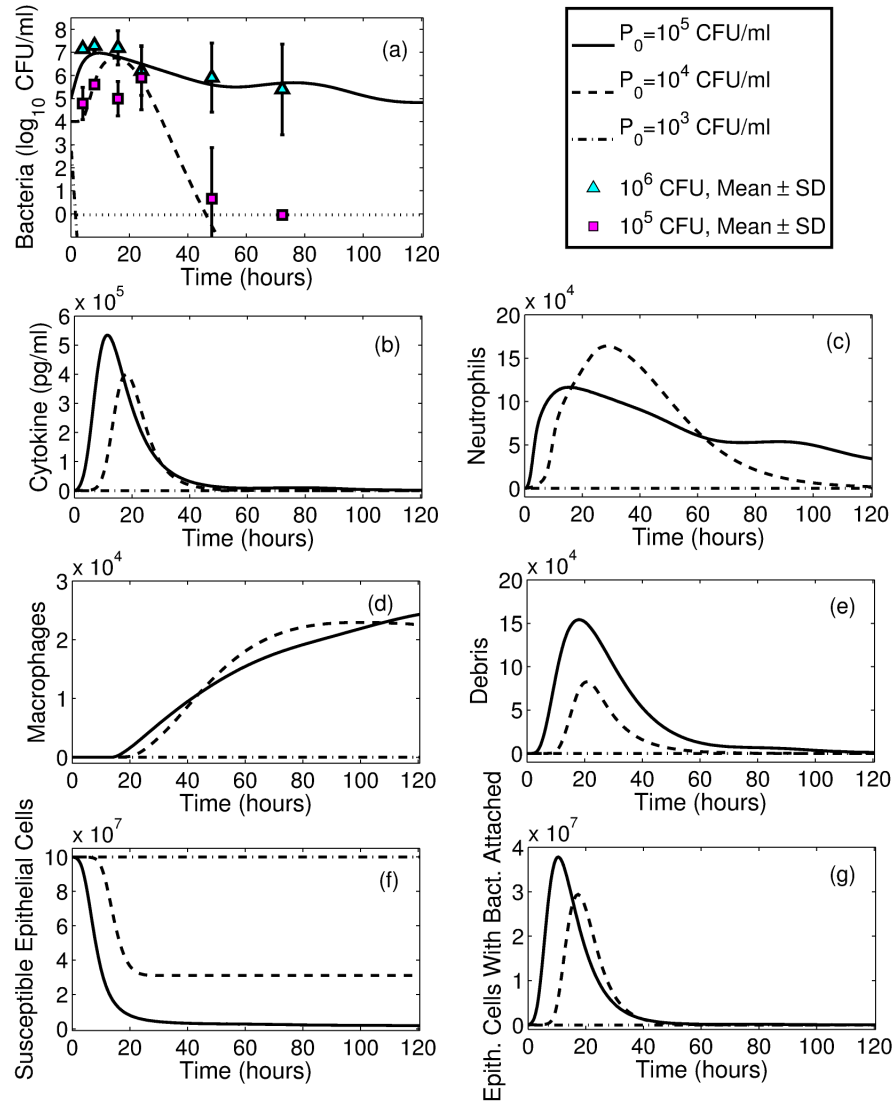


Figure 6: Numerical simulation of the monocyte-derived macrophage model, Equations (12)-(18), using initial conditions  $P_0 = 10^3$  CFU/ml (dashed-dotted line),  $P_0 = 10^4$  CFU/ml (dashed line),  $P_0 = 10^5$  CFU/ml (solid line), and parameter values in Table 3. (a) Bacteria against titer data (squares -  $10^5$  CFU/mouse, triangles -  $10^6$  CFU/mouse), (b) proinflammatory cytokine, (c) neutrophils, (d) monocyte-derived macrophages, (e) debris, (f) susceptible epithelial cells and (g) epithelial cells with bacteria attached.

numbers of pneumococci ( $10^5$  CFU/ml), these cells continue to increase until a peak is reached 9 days pi (not shown in Figure 6), reducing pneumococcus numbers without achieving complete clearance. This extended infection with the resulting prolonging of the neutrophil response (Figure 6c) indicates significant inflammation.

The complexity of our model restricts our ability to fully investigate individual parameter values; however, perturbations in many of the model parameters may significantly influence the dynamics of each stage and reflect differences in the host and the pathogen. Performing a differential sensitivity analysis (see (Bortz and Nelson, 2004; Eslami, 1994; Frank, 1978)) highlights several important aspects of the dynamics (details in the Supplementary File).

Changes in bacterial clearance can be the driving force behind a rapid and favorable resolution. As such, altering either of the two of the parameters controlling clearance,  $\gamma_N$  and  $\gamma_m$ , influences the dynamics. The importance of neutrophils in the early stages of bacterial control is confirmed by the differences observed early in the infection with changes in the rate of bacterial clearance by neutrophils ( $\gamma_N$ ) (Supplementary Figures S1 and S2). Furthermore, this effect is more pronounced and for high initial inocula (i.e.,  $P_0 = 10^5$  CFU/ml). On the other hand, changes in the rate of bacterial clearance by macrophages ( $\gamma_m$ ) influences dynamics later in the infection and to a lesser extent (Supplementary Figures S5 and S6), with little effect when  $P_0 = 10^4$  CFU/ml. In general, parameters related to recruited macrophages ( $\gamma_m$ ,  $\xi$

and  $\tau$ ) are relatively insensitive to changes with intermediate or low initial values of pneumococci since these cells only aid bacterial clearance later in the infection when bacteria is low.

Perturbing factors related to inflammation can also result in dynamical differences. One important parameter with the ability to alter infection kinetics is the rate of neutrophil apoptosis due to bacterial cytotoxicity ( $d_{NP}$ ). However, for high initial inocula, the kinetic effect of an increase in this parameter can be balanced with an increase in the rate of neutrophil recruitment ( $\eta$ ) (Supplementary Figure S1). Other parameters pertaining to inflammation are those which control debris ( $\rho_1, \rho_2, \rho_3, d_D$  and  $k_D$ ), but these parameters are insensitive for both intermediate (except  $k_D$ ) and high initial initial inocula (Supplementary Figures S7 and S8).

#### 4. Discussion

When a pneumococcal infection overcomes the innate immune defenses, bacterial pneumonia can result. There are many factors, including virulence of bacterial strain and host defense status, that determine the eventual outcome of a bacterial challenge to the lung. Developing a basic model of acute pulmonary bacterial infection kinetics that could then be expanded or modified to address specific bacterial pathogens would be ideal. However, establishing the appropriate simplifications to be made is challenging and no generalized model may be sufficient given the variability of immune control and modulation by different bacterial species.

We developed a series of models to gain a deeper understanding of how the different layers of host defense in the lower respiratory tract, including physical barriers, resident cells and recruited cells, combine to fight a pneumococcal lung infection and to address the two thresholds observed given the inoculum size: establishment and eradication. Through our experiments and models, we were able to successfully capture the qualitative behavior of the data and identify key steps.

The initial dose threshold was evident through use of a single equation that took into account a decrease in phagocytosis by alveolar macrophages as bacterial numbers increase, consistent with the view that these cells are sufficient to clear only small densities of pneumococci. Following the first few hours of infection, more complicated dynamics occur. With the neutrophil model, both clearance or sustained growth of bacteria are possible and are dependent on whether alveolar macrophages are engaged in phagocytosis or debris removal, which was correlated to the amount of pneumococcal-induced neutrophil apoptosis. Thus, alveolar macrophages may play a critical role in both establishment and complete eradication of a bacterial infection.

While the neutrophil response is rapid, pneumococcal-induced apoptosis of these cells could result in an equally rapid contraction phase. Normal resolution in the lung includes the apoptosis of neutrophils, but this may also be a significant source of inflammation if the debris is not efficiently cleared. Furthermore, the effects of neutrophil death can be negated with an increase in neutrophil recruitment, but these events combined may still be



harmful even though bacterial numbers would not be affected. This effect is further enhanced with the appearance of macrophages, which contribute to both bacterial clearance and respiratory tract inflammation.

Understanding the ways that damage to the respiratory tract epithelium is accrued during an infection has implications on selecting an appropriate antimicrobial for treatment. The strategy of rapid pathogen lysis by antibiotics may work against immune controls by amplifying inflammatory process leading to adverse outcomes. Cell lysis results in the release of bacterial products (e.g., cytotoxins, DNA, and cell-wall components) which are recognized by the innate immune system and trigger inflammation (McCullers and Tuomanen, 2001; Orman and English, 2000). Therefore, nonlytic antibiotics may improve the outcome possibly by exhibiting antiinflammatory activities that complement the antimicrobial actions (Ivetić Tkalčević et al., 2006). Although we did not study the implications of antibiotics or the complete feedback of damage to the cellular response, our model could be extended to find alternative treatment strategies that effectively eliminate pathogens without increasing pathogenesis.

The signal triggering the macrophage influx into the lung has yet to be fully understood. Delayed macrophage recruitment following neutrophils can predict the behavior of pneumococcus in mice suggesting that an intermediate variable may be responsible. Our model generates consistent results by assuming that the signal originates from neutrophils. However, this is likely an oversimplification and further experiments would be necessary to be sure.

The phagocytic response is essential for successful clearance; however, other factors may contribute to pneumococcal removal. For example, a polysaccharide capsule renders this bacterium resistant to engulfment by phagocytic cells, but antibodies bound to the polysaccharide negate this effect by acting as ligands between the bacteria and phagocyte thereby increasing phagocytic efficiency (van Dam et al., 1990). Furthermore, antibodies activate the classical complement pathway (Paterson and Mitchell, 2006), which is thought to be a key step leading to elimination of pneumococci (Kerr et al., 2005). More recent evidence suggests that IL-17-secreting CD4<sup>+</sup> T-cells are involved in the neutrophil-mediated immune response and may also help prevent colonization (Lu et al., 2008). However, relatively little is known regarding the influence of these cells, which may have only minimal effects on an initial infection in a naive individual.

Much remains to be discovered concerning the properties of bacterial rise, dissemination, and clearance within a host. Mathematical models provide a means of evaluating relative contributions of individual immune components to the processes during a bacterial infection with pneumococci. Using theoretical analyses to compare host responses in different patient populations will help determine why some individuals never get sick while others are easily colonized. Even models with moderate complexity like ours are important tools for the assessment of host responses. As more data becomes available, model formulations can become more refined and parameter values can be estimated thus facilitating an in depth understanding of the underlying biology

of pneumococcal infections.

## 5. Acknowledgements

This material is based upon work supported by the National Science Foundation under grant DMS-0354259 (AMS), NIH contract N01-AI-50020 (AMS), the 21st Century Science Initiative Grant from the James S. McDonnell Foundation (AMS, FRA), and PHS grant AI-66349 and ALSAC (JAM). Portions were done under the auspices of the US Department of Energy (AMS).

## References

- Adamson, I., Young, L., Bowden, D., 1988. Relationship of alveolar epithelial injury and repair to the induction of pulmonary fibrosis. *Am. J. Pathol.* 130, 377–383.
- Austrian, R., 1986. Some aspects of the pneumococcal carrier state. *J. Antimicrob. Chemother.* 18, 35.
- Benton, K., Everson, M., Briles, D., 1995. A pneumolysin-negative mutant of *Streptococcus pneumoniae* causes chronic bacteremia rather than acute sepsis in mice. *Inf. Immun.* 63, 448–455.
- Bergeron, Y., Ouellet, N., Deslauriers, A., Simard, M., Olivier, M., Bergeron, M., 1998. Cytokine kinetics and other host factors in response to pneumococcal pulmonary infection in mice. *Infect. Immun.* 66, 912–922.

- Bingisser, R., Holt, P., 2001. Immunomodulating mechanisms in the lower respiratory tract: nitric oxide mediated interactions between alveolar macrophages, epithelial cells, and T-cells. *Swiss Med. Wkly* 131, 171–179.
- Bortz, D., Nelson, P., 2004. Sensitivity analysis of a nonlinear lumped parameter model of HIV infection dynamics. *Bull. Math. Biol.* 66, 1009–1026.
- Cassatella, M., 1995. The production of cytokines by polymorphonuclear neutrophils. *Immunol. Today* 16, 21–26.
- Clawson, C., Repine, J., 1976. Quantitation of maximal bactericidal capability in human neutrophils. *J. Lab. Clin. Med.* 88, 316–327.
- Cogle, J., Tarling, J., 1982. Cell kinetics of pulmonary alveolar macrophages in the mouse. *Cell Prolif.* 15, 139–143.
- Cogle, J., Tarling, J., 1984. The proliferation kinetics of pulmonary alveolar macrophages. *J. Leukoc. Biol.* 35, 317–327.
- van Dam, J., Flier, A., Snippe, H., 1990. Immunogenicity and immunochemistry of *Streptococcus pneumoniae* capsular polysaccharides. *Antonie van Leeuwenhoek* 58, 1–47.
- DeLeo, F., 2004. Modulation of phagocyte apoptosis by bacterial pathogens. *Apoptosis* 9, 399–413.
- Dockrell, D., Lee, M., Lynch, D., Read, R., 2001. Immune-mediated phago-

cytosis and killing of *Streptococcus pneumoniae* are associated with direct and bystander macrophage apoptosis. *J. Infect. Dis.* 184, 713–722.

Dockrell, D., Marriott, H., Prince, L., Ridger, V., Ince, P., Hellewell, P., Whyte, M., 2003. Alveolar macrophage apoptosis contributes to pneumococcal clearance in a resolving model of pulmonary infection. *J. Immunol.* 171, 5380–5388.

Doherty, D., Downey, G., Worthen, G., Haslett, C., Henson, P., 1988. Monocyte retention and migration in pulmonary inflammation: Requirement for neutrophils. *Lab. Investig.* 59, 200–213.

Duong, M., Simard, M., Bergeron, Y., Bergeron, M., 2001. Kinetic study of the inflammatory response in *Streptococcus pneumoniae* experimental pneumonia treated with the ketolide HMR 3004. *Antimicrob. Agents Chemother.* 45, 252–262.

Eslami, M., 1994. *Theory of Sensitivity in Dynamic Systems: An Introduction.* Springer-Verlag, Berlin.

Fillion, I., Ouellet, N., Simard, M., Bergeron, Y., Sato, S., Bergeron, M., 2001. Role of chemokines and formyl peptides in pneumococcal pneumonia-induced monocyte/macrophage recruitment. *J. Immunol.* 166, 7353–7361.

Frank, P., 1978. *Introduction to System Sensitivity Theory.* Academic Press, Inc., New York, NY.

- Franke-Ullmann, G., Pfortner, C., Walter, P., Steinmuller, C., Lohmann-Matthes, M., Kobzik, L., 1996. Characterization of murine lung interstitial macrophages in comparison with alveolar macrophages in vitro. *J. Immunol.* 157, 3097–3104.
- Giebink, G., 2001. The prevention of pneumococcal disease in children. *New Engl. J. Med.* 345, 1177–1183.
- Gloff, C., Wills, R., 1992. Pharmacokinetics and Metabolism of Therapeutic Cytokines, in: Ferraiolo, B., Mohler, M., Gloff, C. (Eds.), *Protein Pharmacokinetics and Metabolism*. Plenum Press, New York, pp. 127–150.
- Godleski, J., Brain, J., 1972. The origin of alveolar macrophages in mouse radiation chimeras. *J. Exp. Med.* 136, 630–643.
- Gordon, S., Irving, G., Lawson, R., Lee, M., Read, R., 2000. Intracellular trafficking and killing of *Streptococcus pneumoniae* by human alveolar macrophages are influenced by opsonins. *Infect. Immun.* 68, 2286–2293.
- Gwinn, M., Vallyathan, V., 2006. Respiratory burst: Role in signal transduction in alveolar macrophages. *J. Toxicol. Environ. Health B* 9, 27–39.
- Hampton, M., Vissers, M., Winterbourn, C., 1994. A single assay for measuring the rates of phagocytosis and bacterial killing by neutrophils. *J. Leukoc. Biol.* 55, 147–152.
- Henderson, R., Hobbs, J., Mathies, M., Hogg, N., 2003. Rapid recruitment

of inflammatory monocytes is independent of neutrophil migration. *Blood* 102, 328–335.

Ivetić Tkalčević, V., Bošnjak, B., Hrvačić, B., Bosnar, M., Marjanović, N., Ferenčić, Ž., Šitum, K., Čulić, O., Parnham, M., Eraković, V., 2006. Anti-inflammatory activity of azithromycin attenuates the effects of lipopolysaccharide administration in mice. *Eur. J. Pharmacol.* 539, 131–138.

Jones, M., Simms, B., Lupa, M., Kogan, M., Mizgerd, J., 2005. Lung NF- $\kappa$ B activation and neutrophil recruitment requires IL-1 and TNF receptor signaling during pneumococcal pneumonia. *J. Immunol.* 175, 7530–7535.

Jonsson, S., Musher, D., Chapman, A., Goree, A., Lawrence, E., 1985. Phagocytosis and killing of common bacterial pathogens of the lung by human alveolar macrophages. *J. Infect. Dis.* 152, 4–13.

Kadioglu, A., Andrew, P., 2004. The innate immune response to pneumococcal lung infection: The untold story. *Trends Immunol.* 25, 143–149.

Kadioglu, A., Gingles, N., Grattan, K., Kerr, A., Mitchell, T., Andrew, P., 2000. Host cellular immune response to pneumococcal lung infection in mice. *Infect. Immun.* 68, 492–501.

Kadioglu, A., Weiser, J., Paton, J., Andrew, P., 2008. The role of *Streptococcus pneumoniae* virulence factors in host respiratory colonization and disease. *Nat. Rev. Microbiol.* 6, 288–301.

- Kaplanski, G., Marin, V., Montero-Julian, F., Mantovani, A., Farnarier, C., 2003. IL-6: A regulator of the transition from neutrophil to monocyte recruitment during inflammation. *Trends Immunol.* 24, 25–29.
- Kerr, A., Paterson, G., Riboldi-Tunncliffe, A., Mitchell, T., 2005. Innate immune defense against pneumococcal pneumonia requires pulmonary complement component C3. *Infect. Immun.* 73, 4245–4252.
- Knapp, S., Leemans, J., Florquin, S., Branger, J., Maris, N., Pater, J., van Rooijen, N., van der Poll, T., 2003. Alveolar macrophages have a protective antiinflammatory role during murine pneumococcal pneumonia. *Am. J. Respir. Crit. Care Med.* 167, 171–179.
- Lauffenburger, D., 1985. Mathematical analysis of the macrophage response to bacterial challenge in the lung, in: van Furth, R. (Ed.), *Mononuclear Phagocytes: Characteristics, Physiology and Function*. Martinus Nijhoff Publishers, The Netherlands, pp. 351–357.
- Lu, Y., Gross, J., Bogaert, D., Finn, A., Bagrade, L., Zhang, Q., Kolls, J., Srivastava, A., Lundgren, A., Forte, S., et al., 2008. Interleukin-17A mediates acquired immunity to pneumococcal colonization. *PLoS Pathog.* 4, e1000159.
- Malech, H., 2007. Role of neutrophils in the immune system, in: Quinn, M., Deleo, F., Bokoch, G. (Eds.), *Neutrophil Methods and Protocols*. Humana Press, pp. 3–14.



- Marriott, H., Ali, F., Read, R., Mitchell, T., Whyte, M., Dockrell, D., 2004. Nitric oxide levels regulate macrophage commitment to apoptosis or necrosis during pneumococcal infection. *FASEB J.* 18, 1126–1128.
- Maus, U., Srivastava, M., Paton, J., Mack, M., Everhart, M., Blackwell, T., Christman, J., Schlondorff, D., Seeger, W., Lohmeyer, J., 2004. Pneumolysin-induced lung injury is independent of leukocyte trafficking into the alveolar space. *J. Immunol.* 173, 1307–1312.
- McCullers, J., Bartmess, K., 2003. Role of neuraminidase in lethal synergism between influenza virus and *Streptococcus pneumoniae*. *J. Infect. Dis.* 187, 1000–1009.
- McCullers, J., English, B., 2008. Improving therapeutic strategies for secondary bacterial pneumonia following influenza. *Future Microbiol.* 3, 397–404.
- McCullers, J., Tuomanen, E., 2001. Molecular pathogenesis of pneumococcal pneumonia. *Front. Biosci.* 6, D877–89.
- McRitchie, D., Isowa, N., Edelson, J., Xavier, A., Cai, L., Man, H., Wang, Y., Keshavjee, S., Slutsky, A., Liu, M., 2000. Production of tumour necrosis factor  $\alpha$  by primary cultured rat alveolar epithelial cells. *Cytokine* 12, 644–654.
- Mizgerd, J., Meek, B., Kutkoski, G., Bullard, D., Beaudet, A., Doerschuk, C., 1996. Selectins and neutrophil traffic: Margination and *Streptococcus*

pneumoniae-induced emigration in murine lungs. *J. Exp. Med.* 184, 639–645.

Monton, C., Torres, A., 1998. Lung inflammatory response in pneumonia. *Monaldi Arch. Chest Dis.* 53, 56–63.

Murphy, J., Summer, R., Wilson, A., Kotton, D., Fine, A., 2008. The prolonged life-span of alveolar macrophages. *Am. J. Respir. Cell Mol. Biol.* 38, 380–385.

Onofrio, J., Toews, G., Lipscomb, M., Pierce, A., 1983. Granulocyte-alveolar-macrophage interaction in the pulmonary clearance of *Staphylococcus aureus*. *Am. Rev. Respir. Dis.* 127, 335–341.

Orihuela, C., Tuomanen, E., 2006. *Streptococcus pneumoniae*: Invasion and inflammation, in: Fischetti, V., Novick, R., Ferretti, J. (Eds.), *Gram-positive Pathogens*. ASM Press, Am. Soc. Microbiol., Washington, DC, 2nd edition. pp. 253–267.

Orman, K., English, B., 2000. Effects of antibiotic class on the macrophage inflammatory response to *Streptococcus pneumoniae*. *J. Infect. Dis.* 182, 1561–1565.

van Oud Alblas, A., van Furth, R., 1979. Origin, Kinetics, and characteristics of pulmonary macrophages in the normal steady state. *J. Exp. Med.* 149, 1504–1518.

- Paterson, G., Mitchell, T., 2006. Innate immunity and the pneumococcus. *Microbiol.* 152, 285–293.
- Pilyugin, S., Antia, R., 2000. Modeling immune responses with handling time. *Bull. Math. Biol.* 62, 869–890.
- van der Poll, T., Marchant, A., Keogh, C., Goldman, M., Lowry, S., 1996. Interleukin-10 impairs host defense in murine pneumococcal pneumonia. *J. Infect. Dis.* 174, 994–1000.
- Ramphal, R., Small, P., Shands Jr, J., Fischlschweiger, W., Small Jr, P., 1980. Adherence of *Pseudomonas aeruginosa* to tracheal cells injured by influenza infection or by endotracheal intubation. *Infect. Immun.* 27, 614–619.
- Reynolds, A., Rubin, J., Clermont, G., Day, J., Vodovotz, Y., Bard Ermentrout, G., 2006. A reduced mathematical model of the acute inflammatory response: I. Derivation of model and analysis of anti-inflammation. *J. Theor. Biol.* 242, 220–236.
- Rudnev, S., Romanyukha, A., 1995. Mathematical modeling of immune-inflammatory reaction in acute pneumonia. *J. Biol. Sys.* 3, 429–439.
- Schluger, N., Rom, W., 1997. Early responses to infection: Chemokines as mediators of inflammation. *Curr. Opin. Immunol.* 9, 504–508.
- Stadnyk, A., 1994. Cytokine production by epithelial cells. *FASEB J.* 8, 1041–1047.

- Stone, K., Mercer, R., Gehr, P., Stockstill, B., Crapo, J., 1992. Allometric relationships of cell numbers and size in the mammalian lung. *Am. J. Respir. Cell Mol. Biol.* 6, 235.
- Sun, K., Metzger, D., 2008. Inhibition of pulmonary antibacterial defense by interferon- $\gamma$  during recovery from influenza infection. *Nat. Med.* 14, 558–564.
- Tarling, J., Lin, H., Hsu, S., 1987. Self-renewal of pulmonary alveolar macrophages: Evidence from radiation chimera studies. *J. Leukoc. Biol.* 42, 443–446.
- Taut, K., Winter, C., Briles, D., Paton, J., Christman, J., Maus, R., Baumann, R., Welte, T., Maus, U., 2008. Macrophage turnover kinetics in the lungs of mice infected with *Streptococcus pneumoniae*. *Am. J. Respir. Cell Mol. Biol.* 38, 105.
- Taylor, P., Martinez-Pomares, L., Stacey, M., Lin, H., Brown, G., Gordon, S., 2005. Macrophage receptors and immune recognition. *Annu. Rev. Immunol* 23, 901–944.
- Thomassen, M., Buhrow, L., Connors, M., Takao Kaneko, F., Erzurum, S., Kavuru, M., 1997. Nitric oxide inhibits inflammatory cytokine production by human alveolar macrophages. *Am. J. Respir. Cell Mol. Biol.* 17, 279–283.

- Todar, K., 2002. *Streptococcus pneumoniae*: Pneumococcal pneumonia. To-  
dar's Online Textbook of Bacteriology .
- Toews, G., Gross, G., Pierce, A., 1979. The relationship of inoculum size to  
lung bacterial clearance and phagocytic cell response in mice. *Am. Rev.  
Respir. Dis.* 120, 559–566.
- World Health Organization, 2008. *Streptococcus pneumoniae* (pneumococ-  
cus). <http://www.who.int/nuvi/pneumococcus/en/>.
- Zhang, P., Summer, W., Bagby, G., Nelson, S., 2000. Innate immunity and  
pulmonary host defense. *Immunol. Rev.* 173, 39–51.
- Zysk, G., Bejo, L., Schneider-Wald, B., Nau, R., Heinz, H., 2000. Induc-  
tion of necrosis and apoptosis of neutrophil granulocytes by *Streptococcus  
pneumoniae*. *Clin. Exper. Immunol.* 122, 61–66.